Amplitude-preserving finite-difference migration based on a least-squares formulation in the frequency domain

René-Edouard Plessix and Wim Mulder, Shell International E&P, The Netherlands

Summary

A migration algorithm based on the least-squares formulation will reconstruct the correct relative reflector amplitudes only if proper migration weights are applied. These migration weights should approximate the pseudo-inverse of the Hessian of the least-squares error functional that measures the difference between observed and modeled data. Common diagonal approximations are based on the assumption of continuous source and receiver coverage with infinite extent and may lead to poor amplitude estimates for deep reflectors. Here, two new amplitude-preserving migration formulae are derived from a Born approximation of the Hessian that avoids the assumption of infinite continuous coverage. These migration formulae are tested in the context of a frequency-domain finite-difference migration method and provide better relative amplitudes for both shallow and deep reflectors.

Introduction

In the 1980s, it was recognized that depth migration could be seen as an inverse problem. This led to various true-amplitude or amplitude-preserving migration algorithms. Beylkin (1985) derived an amplitude-preserving migration algorithm by viewing migration as an inverse Radon transform under the assumption of infinite and continuous receiver coverage using high-frequency asymptotics. Lailly (1983) and Tarantola (1984) started with a least-squares error functional that measures the difference between measured and modeled data. They found that the gradient of this functional with respect to the underlying model corresponds to a migration image. This approach has the advantage that it can be used independently of the numerical scheme that models the synthetic data and independently of the acquisition geometry. Moreover, it differs from the imaging principle (Claerbout, 1971) or Beylkin's approach because it can directly handle the full data set and does not rely on a particular sorting, such as shot- or offset-gathers.

The gradient of the least-squares functional poorly restores the relative amplitudes of the reflectors. Amplitude-preserving migration is obtained by scaling the gradient with a suitable preconditioner. The optimal preconditioner corresponds to the pseudo-inverse of the Hessian of the least-squares functional. For high-frequency asymptotics and with infinite and continuous source and receiver coverage, the Hessian is a diagonal matrix. With a finite aperture and band-limited data, this is no longer true.

In practice, the Hessian is too large to be used and is therefore approximated by a diagonal or nearly diagonal matrix. If wave propagation is modeled by high-frequency asymptotics using ray tracing, its diagonal and even some off-diagonals are readily computed feasible (Chavent and Plessix, 1999). With a finite-difference scheme for wave propagation, the Hessian can only be computed for small examples and is therefore usually approximated by a diagonal matrix, despite the fact that the Hessian is not diagonally dominant.

For shot-based migration, a common diagonal approximation is the square of the wave field that has been forward-propagated from the source. The resulting formula is similar to the classic imaging principle as used in reverse-time migration. Here we propose two approximations to the diagonal of the Hessian that are based on the full data set, that is, all shots rather than one shot at the time. We use the *linearized* constant-density acoustic wave equation, also known as the Born approximation, to derive the formulae in the context of a frequency-domain finite-difference method.

The paper is organized as follows. First, an analytical expression for the Hessian is derived from the Born approximation of constant-density acoustic wave equation. Further assumptions are required to obtain an approximation by a diagonal matrix. If a continuous and infinite receiver coverage is assumed, we obtain a result similar to the imaging principle. If we assume that shot and receiver positions coincide, a new formula is obtained that is suitable for land-type or in-line Ocean Bottom Cable (OBC) acquisition geometries. An alternative formula is obtained by using a constant-velocity approximation for the back-propagated wave field. These two formulae are tested on synthetic examples using a frequency-domain finite-difference migration algorithm.

Theory

The least-squares error functional J that measures the difference between observed data d and modeled data c for model parameters $r(\mathbf{x})$, is given by

$$J(r) = \tfrac{1}{2}\left\| c(r) - d \right\|^2 .$$

The gradient of the functional with respect to the model parameters is dJ/dr. The migration image is defined by

$$m = -\mathbf{K}\frac{dJ}{dr} ,$$

where $\mathbf{K}$ is a preconditioner, a positive-definite matrix. To find this preconditioner, we derive the Hessian of the least-squares functional for the Born approximation of the constant-density wave equation in the frequency domain. The latter is given by the system of equations

$$L_0 u_0 = f_s / \omega^2 \text{ and } L_0 u_1 = 2\sigma_0^2 r \omega^2 u_0 ,$$

where $L_0 = -\sigma_0^2\omega^2 - \Delta$ is the constant-density wavefield operator for a slowness model $\sigma_0(\mathbf{x})$, ω the angular frequency, Δ the Laplace operator, and $f_s(\omega,\mathbf{x})$ a source term. The slowness model $\sigma_0(\mathbf{x})$ is assumed to be given. The reflectivity $r(\mathbf{x})$ is defined by $r = (\sigma/\sigma_0) - 1$ and represents the unknowns. The pressure field $u = u_0 + u_1$ is the sum of the incident and the scattered field. The synthetic data are for a source located at $\mathbf{x}_s$ are

$$c(\mathbf{x}_s, \mathbf{x}_r) = R(\mathbf{x}_r)(u_0(\mathbf{x}_s) + u_1(\mathbf{x}_s)) ,$$

with R a projection operator onto the receiver position $\mathbf{x}_r$. Using the Green function G of the operator L_0, the modeled data can be expressed as

$$c(\mathbf{x}_s, \mathbf{x}_r, \omega, r) = 2\sum_\omega \sum_\mathbf{x} \sigma_0^2(\mathbf{x}) r(\mathbf{x}) G(\mathbf{x}_s, \mathbf{x}, \omega) G(\mathbf{x}, \mathbf{x}_r, \omega) f_s(\omega),$$

where $\mathbf{x}$ denotes a scattering point in the subsurface. The Hessian corresponds to the second derivative of J with respect to r. Its diagonal is given by

$$H(\mathbf{x},\mathbf{x}) = 4\sum_\omega \sigma_0^4 \sum_{\mathbf{x}_s} |f_s(\omega)|^2 |G(\mathbf{x}_s,\mathbf{x},\omega)|^2 \sum_{\mathbf{x}_r} |G(\mathbf{x},\mathbf{x}_r,\omega)|^2 ,$$

where we have used the fact that $r = r(\mathbf{x})$. The factor that involves $G(\mathbf{x}_s,\mathbf{x},\omega) f_s(\omega) = u_0$ is needed for the gradient computation and is therefore readily available. This is not true for $G(\mathbf{x},\mathbf{x}_r,\omega)$, because the gradient requires $\sum_{\mathbf{x}_r} G(\mathbf{x},\mathbf{x}_r,\omega) R^T(c-d)$, which can be computed by one backward-propagation. Although it is feasible to compute $G(\mathbf{x},\mathbf{x}_r,\omega)$ for each receiver separately, the cost is generally too high in practice. We will therefore make further assumptions to find a cost-effective approximation.

If we assume an infinite and continuous receiver coverage, the term $\sum_{\mathbf{x}_r} \|G(\mathbf{x},\mathbf{x}_r,\omega)\|^2$ is independent of $\mathbf{x}$, as it corresponds to the geometrical spreading of a plane wave. This leads to the following migration formula, which we call type 1:

$$m^{(1)}(\mathbf{x}) = -\frac{\partial_{r(\mathbf{x})} J(0)}{4\sum_\omega \sigma_0^4 \sum_{x_s} |f_s(\omega)|^2 |G(\mathbf{x}_s,\mathbf{x},\omega)|^2} \qquad (1)$$

For a *single* shot, this formula is similar to the one obtained by the imaging principle, since $G(\mathbf{x}_s,\mathbf{x},\omega)\, f_s(\omega)$ is the incident wave field propagated from the source point $\mathbf{x}_s$. This formula generalizes the image principle to multi-shot data and is similar to the formula proposed by Shin *et al.* (2001). Note that if the source coverage is also continuous with infinite extent, the term $\sum_{\mathbf{x}_s} |f_s(\omega)|^2 |G(\mathbf{x}_s,\mathbf{x},\omega)|^2$ becomes independent of $\mathbf{x}$, since it also corresponds to the propagation of a plane wave. In that case, the gradient correctly images the amplitude without the need for preconditioning. In practice, the assumption of infinite receiver coverage is unrealistic for deep reflectors and will not allow for a correct reconstruction of reflector amplitudes.

To avoid the assumption of infinite coverage without increasing the cost of the preconditioner, we propose two new formulae. First, we assume that the receiver positions more or less coincide with the source positions, so that $\sum_{\mathbf{x}_r} \|G(\mathbf{x},\mathbf{x}_r,\omega)\|^2$ can be replaced by $\sum_{\mathbf{x}_s} \|G(\mathbf{x}_s,\mathbf{x},\omega)\|^2$. This leads to a migration formula that we call type 2:

$$m^{(2)}(\mathbf{x}) = -\frac{\partial_{r(\mathbf{x})} J(0)}{4\sum_\omega \sigma_0^4 \left(\sum_{x_s} |f_s(\omega)|^2 |G(\mathbf{x}_s,\mathbf{x},\omega)|^2 \right)^2} \qquad (2)$$

The assumption is reasonable for land- or OBC-type acquisition geometries.

The second option is to evaluate $\sum_{\mathbf{x}_r} \|G(\mathbf{x},\mathbf{x}_r,\omega)\|^2$ in a constant velocity model assuming continuous coverage between the minimum offset, $x_r^{\min}(\mathbf{x}_s)$, and the maximum offset, $x_r^{\max}(\mathbf{x}_s)$. In two space dimensions, $\sum_{\mathbf{x}_r} \|G(\mathbf{x},\mathbf{x}_r,\omega)\|^2$ becomes proportional to

$$a(\mathbf{x}_s,\mathbf{x}) = \operatorname{asinh}\left(\frac{\mathrm{x}_\mathrm{r}^{\max}(\mathbf{x}_s) - \mathrm{x}}{|\mathrm{z} - \mathrm{z}_\mathrm{r}|}\right) - \operatorname{asinh}\left(\frac{\mathrm{x}_\mathrm{r}^{\min}(\mathbf{x}_s) - \mathrm{x}}{|\mathrm{z} - \mathrm{z}_\mathrm{r}|}\right),$$

with $\mathbf{x} = (x,z)$. Here it is assumed that all receivers are located at the same depth, z_r. We call the resulting migration formula type 3:

$$m^{(3)}(\mathbf{x}) = -\frac{\partial_{r(\mathbf{x})} J(0)}{4\sum_\omega \sigma_0^4 \sum_{x_s} |f_s(\omega)|^2 |G(\mathbf{x}_s,\mathbf{x},\omega)|^2 a(\mathbf{x}_s,\mathbf{x})} . \qquad (3)$$

Note that the formulae (1), (2) and (3) reconstruct only the *relative* amplitudes. In the following examples, the results have been normalized to allow for comparison.

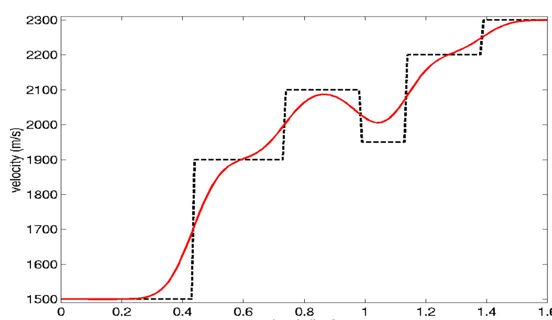

Figure 1: A layered velocity model (dotted blue line) and the smoothed background velocity model (solid red line).

Amplitude preserving finite-difference migration

Example for a 1D model

The first example is based on a horizontally layered model. Figure 1 shows the true velocity model, used to generate the data set, and a smooth version, used as the background velocity model when migrating the data. The data set consists of 62 shots and 63 receivers. The receivers are located between 25 m and 1575 m at a 25-m interval. The shots are located between 32.5 m and 1562.5 m with 25-m interval. This mimics a land-type acquisition geometry. The

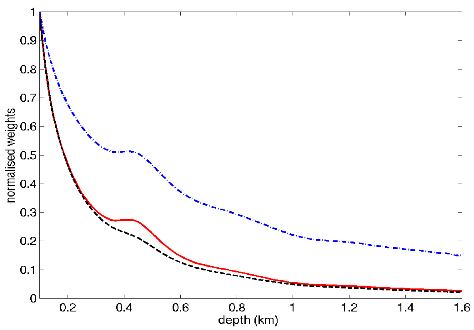

Figure 3: inverse of the preconditioner type 1 (dashed blue line), type 2 (solid red), and type 3 (dotted black line).

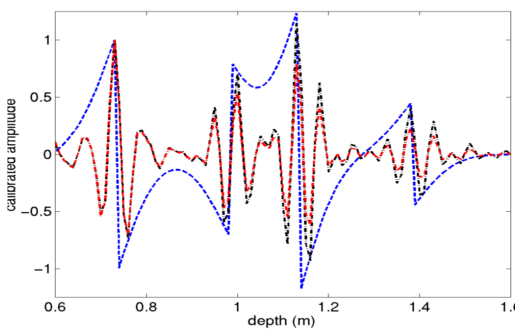

Figure 4: migration results for type 1 (solid red line) and type 3 (dashed black) compared to the true reflectivity (dotted blue).

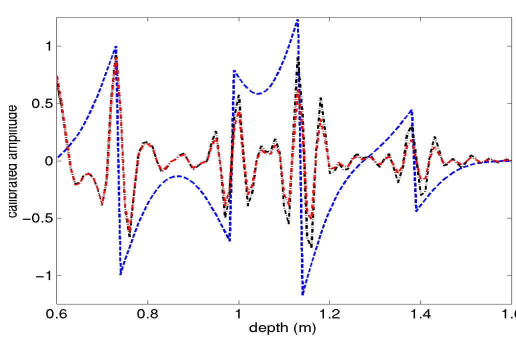

Figure 5: comparison between the true reflectivity (dashed blue) and the type 2 (solid red) and 3 (dashed black) migration results for a marine-type acquisition geometry.

frequency ranges from 15 to 30 Hz.
The preconditioners of type 1, 2, and 3 are plotted in Fig. 2. Whereas the results for type 2 and 3 are almost identical, type 1 shows a different behavior: the deep reflectors are less boosted. This can be seen in Fig. 3 where we have plotted the migration results of type 1 and type 3. The results have been normalized to the second reflector. The amplitudes of the deep reflectors, especially those at 1.15 km and 1.4 km depth, are underestimated by type 1 whereas they are correctly predicted by type 3.
Because the land-type of acquisition geometry leads to nearly identical results for type 2 and 3, we have considered a marine-type acquisition with the same model. Each shot now has 61 receivers with offsets ranging from 75 to 1575 m. The results are displayed in Fig. 4 and suggest a slightly better performance for the migration of type 3.

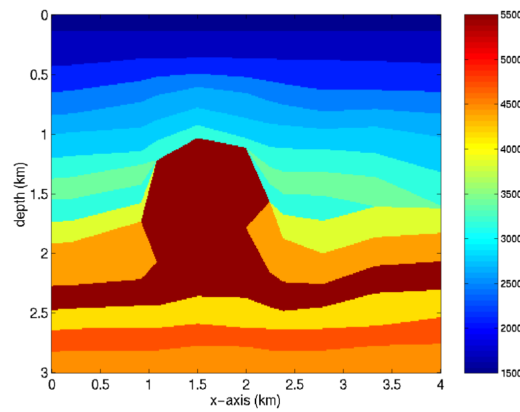

Figure 6: salt dome velocity model

Salt dome example

The second example is a synthetic salt dome model. The velocity model is displayed in Fig. 5. Synthetic data were generated with a time-domain finite-difference code. The

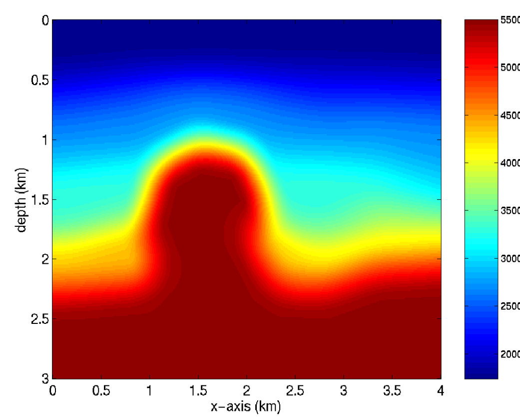

Figure 2: background velocity for the salt dome model

marine-type data set contains 351 shots of 157 receivers each, with a maximum offset of 4 km. After Fourier transformation of the time-domain data, 14 frequency panels were extracted with the frequencies ranging from 18 to 29.7 Hz. For the migration, the background velocity shown in Fig. 6 was used. The true reflectivity is plotted in Fig. 7. The reflectivity obtained by the migration formula (1) is shown in Fig. 8, and by formula (3) in Fig. 9. We observer that the amplitude behavior is better estimated by formula (3) than by formula (1), although the amplitude of the salt dome is still overestimated. This illustrates the limitations of migration weights based on the Born approximation when the velocity contrasts are very large.

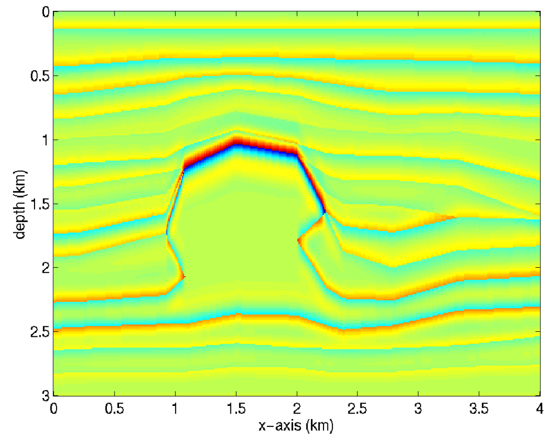

Figure 7: true reflectivity.

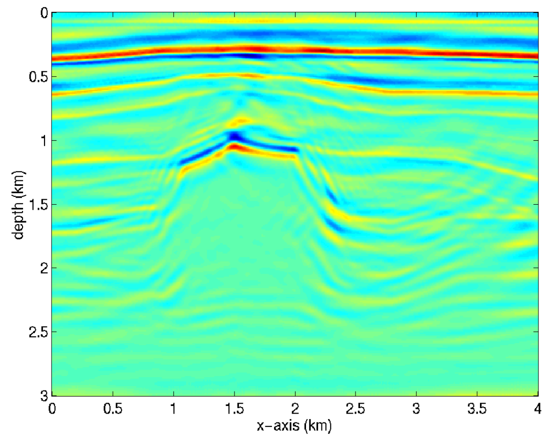

Figure 8: reflectivity obtained with the migration of type 1.

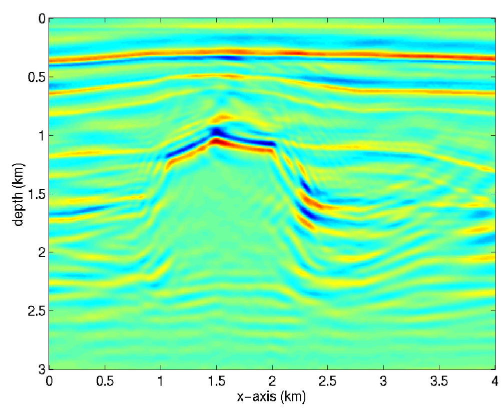

Figure 9: reflectivity obtained with the migration of type 3.

Conclusions

We have derived two new amplitude-preserving finite-difference migration formulae. The migration operator is obtained as the gradient of the least-squares functional, whereas the migration weighting or preconditioner is found by a suitable approximation of its Hessian. The results are different from the classical ones, because they are applied directly to the full data set and not to a particular type of data sorting, such as a shot- or offset-gather. Also, the usual assumption of infinite receiver coverage has been dropped. Numerical examples show that these migration weights better predict the relative amplitudes, especially for deep reflectors.

References

Beylkin, G., 1985, Imaging of discontinuities in the inverse scattering problem by inversion of a causal generalized Radon transform: J. Math. Phys., **26**, 99–108.

Claerbout, J. F., 1971, Toward a unified theory of reflector mapping: Geophysics, **36,** 467–481.

Chavent, G. and Plessix, R.-E., 1999, An optimal true-amplitude least-squares prestack depth-migration operator: Geophysics, **64,** 508–515.

Lailly, P., 1983, The seismic inverse problem as a sequence of before stack migration: In Proc. of Conf. on Inverse Scattering, Theory and Applications, SIAM, Philadelphia.

Shin, C., Jang, S. and Min, D.-J., 2001, Improved amplitude preservation for prestack depth migration by inverse scattering theory: Geophys. Prosp., **49,** 592–606.

Tarantola, A., 1984, Inversion of seismic reflection data in the acoustic approximation: Geophysics, **49,** 1259–1266.